DOI: 10.13009/EUCASS2019-629

Modes Reconstruction of Hybrid Combustion Flame

Anna Petrarolo⋆† *and Mario Kobald*⋆
⋆*German Aerospace Center (DLR), Institute of Space Propulsion, Propellants Department*
Langer Grund, 74239 Hardthausen, Germany
anna.petrarolo@dlr.de · mario.kobald@dlr.de
†Corresponding author

Abstract
Optical investigations of hybrid combustion flame are essential to better understand their combustion mechanism. Therefore, combustion tests using paraffin-based fuels and gaseous oxygen (GOX) were performed in the framework of this research. The combustion flame was analyzed with two decomposition methods, which give a low-dimensional representation of the complex flow structures and identify the main combustion phenomena. To prove the reliability of this analysis, a modes reconstruction has been performed. The results show that the output of the reconstruction provides a good representation of the original combustion video frames. This means that the low-dimensional modes representation is able to efficiently and correctly describe the main combustion phenomena in the combustion chamber.

1. Introduction

Hybrid rocket engines have several advantages compared to classical solid or liquid rockets. Due to the fact that the propellants are stored in two different states of matter, hybrid motors are safer than solids. This also contributes to reduce the total costs of the engine. Moreover, they are characterized by controllable thrust, including shut off and restart capability. With respect to liquid engines, they are mechanically simpler and, consequently, cheaper.[15] Finally, their performance are in between those of solid and liquid engines. However, due to the diffusion limited combustion process typical for this kind of engines (the propellants are not pre-mixed, but they need to gasify and mix with each other before being able to react), hybrid systems using conventional polymeric fuels are characterized by poor regression rate performance (resulting in low thrust level). In order to overcome this problem, the so-called liquefying hybrid rocket fuels, such as paraffin-based ones, can be used. These fast burning fuels are characterized by low viscosity and surface tension and they experience a different combustion mechanism with respect to conventional polymeric fuels.[13] During the combustion, instead of pyrolysing, they form a thin liquid layer on the fuel surface, which becomes unstable due to the high-speed gas flow in the fuel port.[12] The liquid layer instabilities produce, in turn, droplets that entrain in the gas flow, thus working like a spray injection along the length of the motor, see also Fig. 1. This causes an increase in the fuel burning area and, consequently, an increase in the regression rate of the fuel grain. This enables simple, single-port fuel grain designs and makes hybrid propulsion a competitive candidate for launch systems and in-space missions. Unfortunately, the entrainment phenomenon in hybrid rocket combustion process is still a matter of ongoing research and not fully understood yet.

For a better understanding of the combustion process, detailed optical analysis of the burning tests have been performed, see Fig. 2. The combustion process has been recorded with a high-speed video camera that is able to capture 10 000 frames per second. This results in a big amount of data that have to be analyzed. Therefore, it is important to reduce the dimension of the problem such that the essential flow structures can be easily identified. In fact, turbulent and other irregular structures (such as vortices) might exist in the dataset. Even if these structures only exist within a short period of time, they might strongly affect the overall combustion behaviour. Therefore, it is necessary to perform a mode decomposition of the dataset, which is able to detect the main flow structures and strongly irregular combustion phenomena.

In this work, two different decomposition techniques were applied to the analysis of the luminosity field of the combustion process in a hybrid engine: Principal Component Analysis (PCA) and Independent Component Analysis (ICA). In particular, PCA enables the recognition of the main energetic structures of the flow field and the visualization of its relevant morphologies by decomposing it into mean, coherent and incoherent parts via statistical methods. On the other hand, ICA identifies the leading independent structures during the burning process. By comparing the results of the two decomposition methods, valuable insights into the dynamics of the burning process in a hybrid engine can be

DOI: 10.13009/EUCASS2019-629

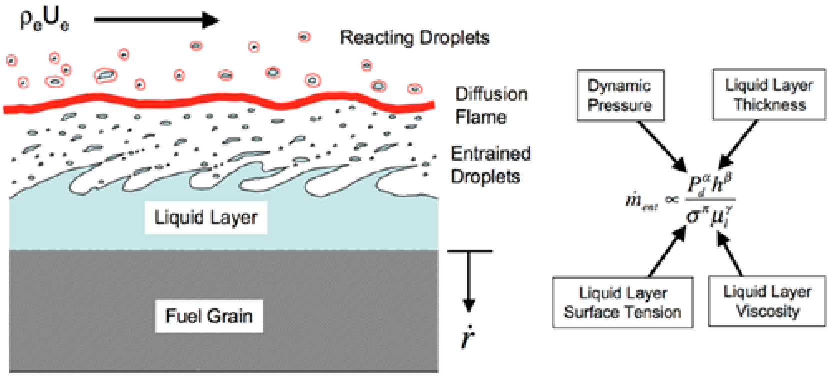

Figure 1: Liquefying fuel combustion theory, taken from Karabeyoglu et al.[11, 14]

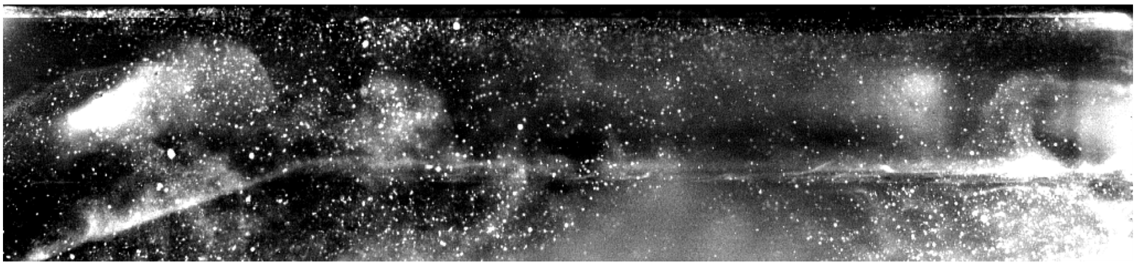

Figure 2: Liquefying fuel combustion image created within this research (oxidizer mass flow from left to right)

obtained. Moreover, in order to prove the validity of the decomposition, a modes reconstruction has been performed. The results show that the output of the reconstruction provides a good representation of the original combustion video frames. This means that the low-dimensional modes representation is able to efficiently and correctly describe the main combustion phenomena in the hybrid engine.

2. Theoretical Background: Decomposition Methods

2.1 Proper Orthogonal Decomposition

The POD (Proper Orthogonal Decomposition) has been used in diverse area of research to obtain approximate, low-dimensional descriptions of turbulent fluid flows, structural vibrations and dynamical systems. It has also been extensively used in image processing, signal analysis and data compression.[5]

The POD is a statistical method where an orthogonal transformation is used to convert a set of data into a set of linearly uncorrelated variables, which are called principal components. Their number is usually less than the number of the original variables. This transformation is performed so that the principal components are sorted by decreasing variance under the constraint that each component has to be orthogonal to the preceding ones, thereby being uncorrelated. An orthogonal transformation to the basis of the eigenvectors of the sample covariance matrix is performed and the data are projected onto the subspace spanned by the eigenvectors corresponding to the largest eigenvalues (most energetic modes). So, POD gives an orthogonal basis that ranks modes according to an energy criterion.[4] This enables us to retain only the dominant modes and to filter out the presence of the measurement noise, thus providing a good characterization of the dynamics of the problem. Finally, POD is able to explicitly separate the spatial and time information.[16] On the other hand, the linear nature of the method can be a restriction for some data sets. Moreover, since POD removes linear correlations among variables (i.e. diagonalizes the covariance matrix), it is only sensitive to second-order statics. This means that this method is able to find only uncorrelated variables.[16]

In the present work, the POD is applied to the analysis of the luminosity field of images (scalar field) in a reactive flow. This allows for an analysis of the considered scalar field by decomposing it into mean, coherent and incoherent parts via statistical methods and to visualize the relevant morphologies. In general, the coherent part includes all fluctuations possessing a somehow structured feature over the burning process. The incoherent part includes all fluctuations for which no pattern can be identified over the burning process. It is commonly thought that the first few modes

DOI: 10.13009/EUCASS2019-629

correspond to the average structure of the data, while higher order modes contain information about fluctuations.[2] The Nonlinear Iterative Partial Least Squares (NIPALS) algorithm is used for the principal component analysis in the POD method. The Power Spectral Density (PSD) of the temporal and spatial coefficients is performed at the end of the algorithm in order to obtain the excited frequencies and wavelengths during the combustion.

2.1.1 Mathematical Background

Consider a data set $u_k(x)$, where x is the space coordinate and k is the snapshot index. This set can be conveniently represented as a matrix $\mathbf{U} \equiv u_{jk}$, where $j = 1, ..., M$ spans the number of space position and $k = 1, ..., N$ spans the number of snapshot u_k. It is possible to build a set

$$\Phi = \varphi_1, \varphi_2, ..., \varphi_N \tag{1}$$

of linear combination of the snapshots

$$\varphi_i(x) = \sum_{k=1}^{N} \psi_{ik} u_k(x) \tag{2}$$

where $\Psi = \psi_1, \psi_2, ..., \psi_N$ is obtained by solving the eigenvalue problem $\mathbf{C}\Psi = \lambda\Psi$, with $\mathbf{C}$ being the space correlation matrix:

$$\mathbf{C} = \frac{1}{N}\mathbf{U}^T\mathbf{U} \tag{3}$$

Then, $u_k(x)$ can be approximated by a linear combination of the first K modes:

$$\tilde{u}_k = \sum_{i=1}^{K} c_{ik}\varphi_i(x) \tag{4}$$

where $K \leq M$ is the number of modes used for truncation and c_{ik} are the modal coefficients that can be determined by projection of the data onto the POD modes.

2.2 Independent Component Analysis

The ICA (Independent Component Analysis) is a statistical signal processing technique whose main applications are blind source separation, blind deconvolution and feature extraction.[9] One application with combustion was demonstrated by Bizon et al.[1,3] They applied ICA to 2D images of combustion-related luminosity, in order to identify leading independent structures.

The ICA is a statistical and computational technique for revealing hidden components that underlie the observed data. The latent variables are assumed to be non-Gaussian and mutually independent in space and/or time: they are called the independent components of the observed data. The transformed variables correspond to the underlying components that describe the essential structure of the data and that correspond to some physical causes involved in the process. The method which is used in this analysis for finding the independent components is the maximization of non-Gaussianity of the sample matrix.[10] Each local maximum or minimum gives one independent component.

The ICA is a much more powerful method with respect to the POD. The basis functions found by the POD, which reflect the directions of the most prominent variances in the data, are uncorrelated but not statistically independent. This means that higher order dependencies still exist and, therefore, they are not properly separated. In other words, all POD modes contain some element of all structures found in all of the fields.[3] On the other hand, ICA is able to search for basis functions that are statistically independent or as independent as possible, increasing the independence to higher statistical orders. When deriving these components, the data are separated into either spatially (sICA) or temporally (tICA) independent components; each choice yields corresponding statistically independent images or time courses. In particular, tICA produces a set of mutually independent temporal sequences and a corresponding set of unconstrained images. sICA determines mutually independent images and a corresponding set of unconstrained temporal sequences,[1,7] see also Fig. 3.

Some weak points have to be highlighted also for ICA: unlike for the principal components of the data, which are ordered according to their variance, no intrinsic order exists for the independent components. Moreover, ICA provides a solution only up to a multiplicative constant. In other words, the order, the signs and the scaling of the independent components cannot be determined: indeterminacy is an inherent property of this analysis.[10]

The aim of the present work is to identify independent spatial structures evolving in time. Therefore, the spatial ICA is applied to the analysis of the luminosity field of the combustion process in a hybrid engine. This allows the

DOI: 10.13009/EUCASS2019-629

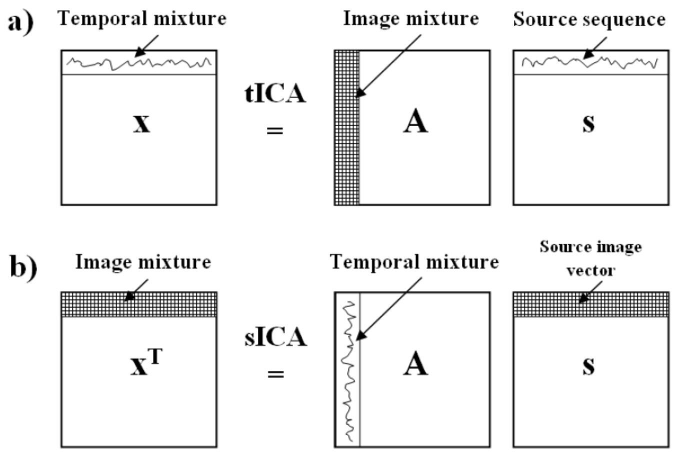

Figure 3: Vector Matrix representation of the mixing process for tICA and sICA, taken from Stone[22]

identification of the leading independent structures during the burning process. The FastICA algorithm[10] is employed. It maximizes non-gaussianity by means of a gradient method, estimated by the absolute value of kurtosis, as a measure of statistical independence. The Power Spectral Density (PSD) of the temporal and spatial coefficients is performed at the end of the algorithm in order to obtain the excited frequencies and wavelengths during the combustion.

2.2.1 Mathematical Background

Consider a vector $\mathbf{x}(t)$ whose elements are the temporal signals mixtures $x_1(t), ..., x_m(t)$ of unknown mutually independent components, i.e. the temporal source signals $s_1(t), ..., s_n(t)$ denoted by the vector $\mathbf{s}(t)$, with $m \geqslant n$. Let us assume $m = n$. Using the vector-matrix notation, the mixing model is written as:

$$\mathbf{x} = \mathbf{A}\mathbf{s} \tag{5}$$

where $\mathbf{A}$ is the so-called mixing matrix, mapping the source signals $\mathbf{s}$ to the mixtures $\mathbf{x}$. The classic problem of ICA consists of estimating both A and $\mathbf{s}$ when only $\mathbf{x}$ is observed. Eq. 5 can be rewritten as:

$$\mathbf{s} = \mathbf{W}\mathbf{x} \tag{6}$$

which can be solved by computing the matrix $\mathbf{W} = \mathbf{A}^{-}1$ in such a way that a linear combination $\mathbf{y} = \mathbf{W}\mathbf{x}$ is the optimal estimation of the independent source signals $\mathbf{s}$. Under the assumption of statistical independence of the components, each of whom characterized by a non-Gaussian distribution, the basic ICA problem given by Eqs. 5 and 6 can be solved by maximization of the statistical independence of the estimates $\mathbf{y}$. Depending on the definition of statistical independence, the most popular ICA algorithms are based on the minimization of mutual information and maximization of non-gaussianity. In this work, a FastICA algorithm[10] is employed, which, by means of a gradient method, maximizes non-gaussianity, estimated by the absolute value of kurtosis or fourth order cumulant, as a measure of statistical independence. The algorithm is applied on centered and whitened image data, by using the transformation:

$$\mathbf{x} = \mathbf{D}^{-0.5}\mathbf{E}^{T}(\mathbf{x}' - E\{\mathbf{x}'\}) \tag{7}$$

where $\mathbf{x}'$ is the raw data, $\mathbf{E}$ is the $n \times n$ matrix made of POD eigenvectors, $\mathbf{D}$ is the diagonal matrix made of POD eigenvalues and $E\{\cdot\}$ is the ensemble average. It must be noted that often the number n of ICs to be determined is smaller than the number m of available signal mixtures. In this case, the plain application of the basic ICA would lead to a non-square $m \times n$ mixing matrix $\mathbf{A}$, whose inverse cannot be determined. One solution is to reduce the rank of the data during the whitening phase, by projecting the observed mixture onto its POD modes and truncating to the few most significant. In this case, $\mathbf{E}$ is the rectangular matrix made of the leading n POD eigenvectors and $\mathbf{D}$ contains the corresponding POD eigenvalues. This preprocessing assures that the algorithm still operates on a square $n \times n$ matrix and, additionally, allows to reduce the noise present in the data.[8]

DOI: 10.13009/EUCASS2019-629

3. Experimental Set-Up and Methods

3.1 Paraffin-Based Fuels

Four different paraffin-based fuels have been investigated in the framework of this research. The wax that has been used as a base for all the fuels is type 6805 from the manufacturer Sasol Wax. It has been chosen because of its viscosity and surface tension values, which are the two fuel parameters that are expected to have the biggest influence on the entrainment process (see also Fig. 1). Detailed laboratory experiments have been performed before, in order to measure these two parameters for the different fuels, see also.[21] All samples for the ballistic tests have been blackened by additives during fabrication to limit radiation effects during combustion to the fuel surface. Generally, the amount of blackening additive was less than 2% and has therefore negligible impact on the performance. Three different percentages of a commonly available polymer have also been added to the paraffin samples, in order to have different viscosity values. In this way it was possible to study the influence of this parameter on the entrainment process.

Moreover, three different fuel configurations have been investigated. Combustion tests with fuel slabs with 5°, 20°and 90° forward facing ramp angle have been performed (see Fig. 4) and the influence of the fuel configurations on the combustion and entrainment process has been investigated.

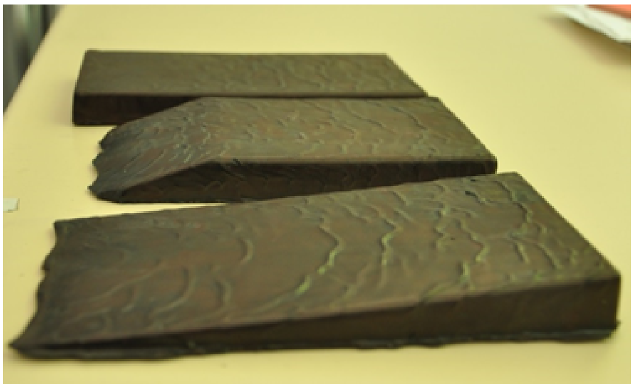

Figure 4: Different fuel configurations used in this research

3.2 Test Set-Up and Data Acquisition

The experimental tests were performed at the Institute of Space Propulsion at the DLR Lampoldshausen at the test complex M11. An already existing modular combustion chamber, used in the past to investigate the combustion behaviour of solid fuel ramjets, was adjusted and used for the test campaigns.[6] A side view of the whole combustion chamber set-up is shown in Fig. 5. The oxidizer main flow is entering the combustion chamber from the left, after having passed two flow straighteners. Its mass flow rate is adjusted by a flow control valve and it is measured with a Coriolis flow meter. Ignition is done via an oxygen/hydrogen torch igniter from the bottom of the chamber. A test sequence is programmed before the test and is run automatically by the test bench control system. More details about the test bench and test settings are given in Kobald et al. and Petrarolo et al.[17,19,21]

In the framework of this research, all tests were done at atmospheric pressure and with an oxidizer mass flow ranging from 10 to 120 g/s. Combustion tests were performed using a single-slab paraffin-based fuel in combination with gaseous oxygen. Three fuel slab configurations with different forward facing ramp angle were tested. Burning time was 3 seconds for each test. For video data acquisition a Photron Fastcam SA 1.1 high speed video camera was used with a maximum resolution of 1024x1024 pixel and a frame rate of 10000 frames per second. Resolution and shutter time of the camera were adjusted for each test, according to the test conditions and position of the camera.

DOI: 10.13009/EUCASS2019-629

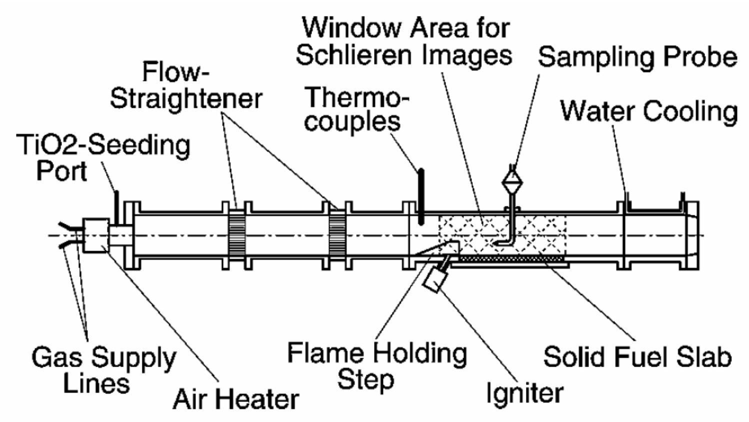

Figure 5: Sideview of the combustion chamber set-up

3.3 Video Analysis

The combustion high-speed videos are analysed with a Matlab® routine, which returns as results the most excited frequencies and wavelengths characterizing the liquid melt layer.

As first step, a video pre-processing is performed, see Fig.6. During this phase, the images are exported from the video and cropped with the Software VirtualDub. Usually filters are added, to adjust the brightness and the contrast of the images. The function sharpen is also used to enhance the contrast of adjacent elements. There exists also lateral burning at the sides of the fuel, so the bottom of the fuel is cropped just up to the solid liquid interface, to reduce noise and errors. Yet, the size of the area of interest is kept as large as possible in order to capture the flow dynamics on the whole upper surface of the fuel slab. The angled front and the rear end, where further vortices are created, are not included in the frames. The images are then exported to Matlab® and converted from true-color RGB to binary data images, based on a luminance threshold. The background noise, which usually consists of small light spots (most likely burning paraffin droplets), is removed. Finally, the waves edge is automatically detected and a sparse matrix is created. Each frame is then rearranged as a column vector and the Snapshot Matrix, which contains all the frames to analyse, is created. It has to be noticed that the recorded video data is a line of sight measurement. Thus, the data in the analysis represent an integrated measurement over the whole fuel slab width. This has to be taken into account when they are analysed. In a second step, the Snapshot Matrix is decomposed with both algorithms, POD and ICA, into two matrices containing spatial and temporal coefficients. At the end, the Power Spectral Density (PSD) of these coefficients is performed, in order to obtain the most excited frequencies and wavelengths during the combustion. Further details of the applied methods are given in Kobald et al.[18] and Petrarolo et al.[19]

4. Results and Discussion

In the framework of this research, the decomposition into principal and independent components of the flame luminosity field in a hybrid rocket combustion chamber was performed. This allowed to recognize the main energetic (with POD) and independent (with ICA) structures characterizing the hybrid combustion flame, depending on the fuel composition and configuration, oxidizer mass flow and combustion chamber pressure (see Petrarolo et al.[20]). In order to prove the validity of the decomposition methods, a modes reconstruction of the hybrid flame was performed in this work. To do so, one combustion test was chosen (see Table 1) and 100 frames (corresponding to 0.01 seconds of burning) taken from its steady-state phase were considered. First, these frames were decomposed into their principal and independent components with POD and ICA. In particular, different numbers of modes were computed, since this parameter has a great influence on the results. Finally, a flame reconstruction using the principal and independent components computed in the first step was performed.
The results show that the output of the reconstruction gives a good representation of the main hybrid combustion flame. This means that the low-dimensional modes representation is an efficient way to describe big dataset, since it is able to capture the main dynamics of the observed phenomenon, without loosing important information but filtering out possible noise sources.

DOI: 10.13009/EUCASS2019-629

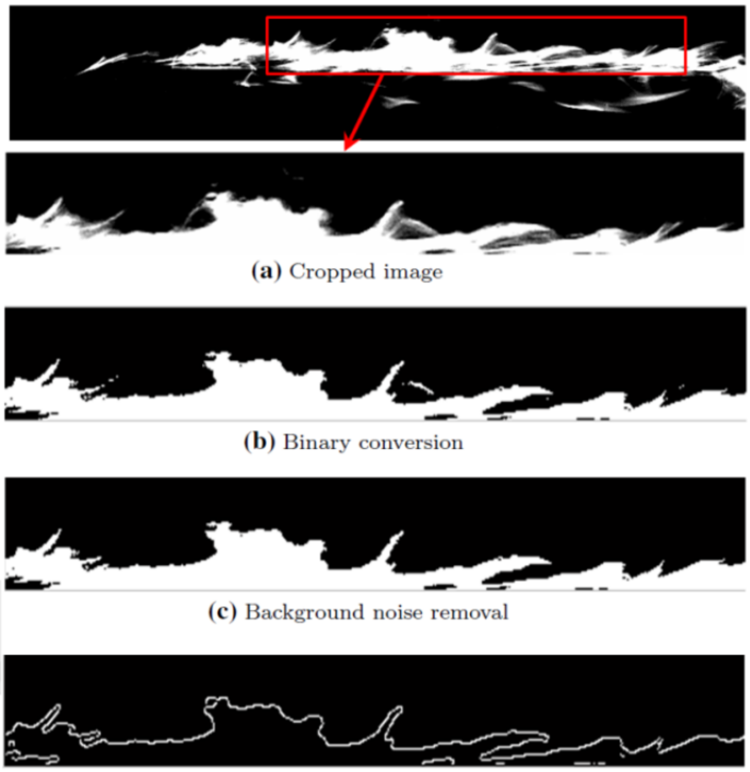

(a) Cropped image

(b) Binary conversion

(c) Background noise removal

(d) Edge detection

Figure 6: Video data pre-processing steps. Taken from[21]

Table 1: Test matrix

Test no.	Fuel Composition	$\dot{m}_{Ox}[g/s]$	Fuel Configuration
203	6805+5%polymer	50	20° ramp

4.1 POD Reconstruction

As said in section 2.1, the POD is basically an eigenvalue decomposition where the data are projected onto the subspace spanned by the eigenvectors corresponding to the largest eigenvalues. Therefore, this method is able to retain the most energetic and dominant modes. In this study, the minimum number of modes to consider in order to correctly describe the dynamics of the phenomenon was computed, according to an energy criterion. In Figures 7 and 8, it is possible to notice that the first eigenvalue carries already almost 90% of the whole energy content of the dataset. Moreover, with only 20 modes, 98% of the total energy has already been retained. This means that it is possible to efficiently describe the dynamics of the combustion with just 20 modes. In order to prove this, 10, 25, 50 and 100 modes were considered in this work, for both the decomposition and the reconstruction.

From the results of the decomposition, it is shown that the average flame structure is already well described by the first mode (see Fig. 9). In fact, no difference can be noticed when 1 or 100 modes are considered. Only smaller turbulent structures and fluctuations, corresponding to higher modes, are better described when more modes are computed. On the other hand, looking at the results of the reconstruction (Fig. 10), it is possible to notice that some differences are visible, depending on the number of modes considered. Of course, when just 1 mode is computed, only the average flame can be reconstructed. All the information about fluctuations, smaller turbulent structures, random appearing vortices and noise are filtered out. If 10 modes are considered, the main flame behaviour and its leading structures are well reproduced, but the flame appears to be flatter than in the original frames. The information about shorter waves are lost: some of them are merged with longer waves, others are levelled with the main flame. The results looks better already with 25 modes. In this case, shorter waves are more clearly detected, but some small waves are

DOI: 10.13009/EUCASS2019-629

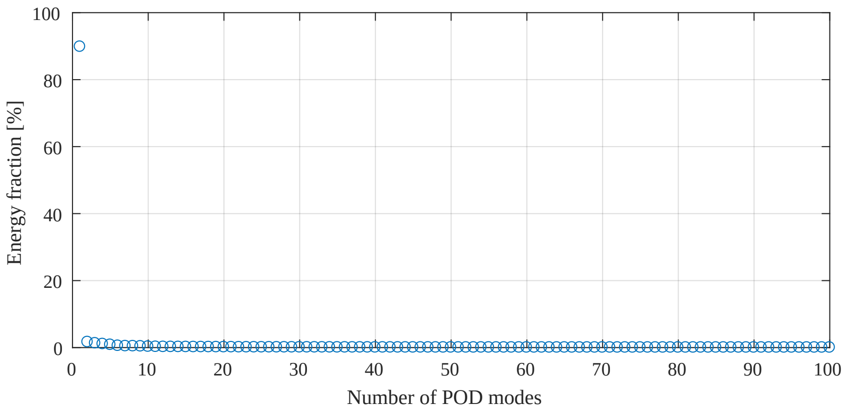

Figure 7: Energy fraction associated to each POD mode

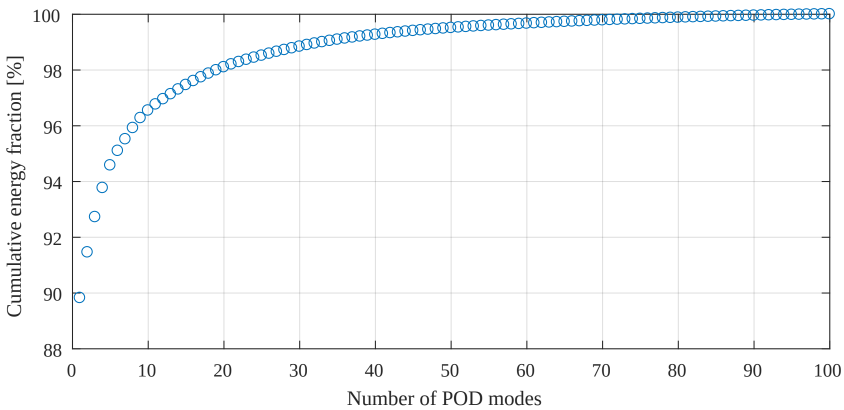

Figure 8: Cumulative energy fraction associated to each POD mode

still merged together, if they are close to each other. No differences are observed between the reconstructions with 50 and 100 modes. In both cases, all waves are clearly recognized and the dynamics is well reproduced. Even droplets are correctly detected and reconstructed.

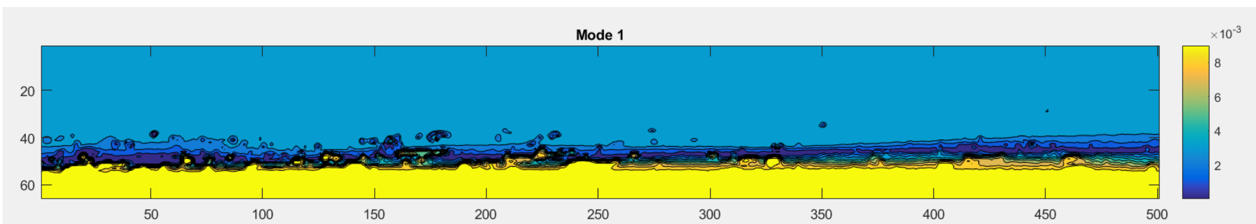

Figure 9: First POD mode, representing the average flame structure

The obtained results show that 10 modes are already enough to correctly describe the main flame dynamics, like average flame shape and height. In fact, 10 modes already retains 97% of the total energy content of the combustion data. If smaller structures (such as shorter waves or droplets) or random appearing dynamics have to be detected, a higher number of modes needs to be considered. In any case, the reconstruction of the POD modes shows that the principal components decomposition is an efficient way to represent the main dynamics and the leading structures of the hybrid combustion process.

DOI: 10.13009/EUCASS2019-629

(a) Frame 20001: original

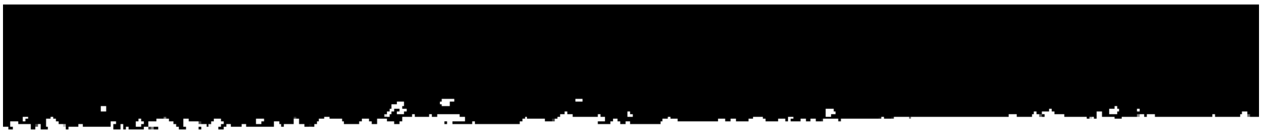

(b) Frame 20001: reconstructed with 1 mode

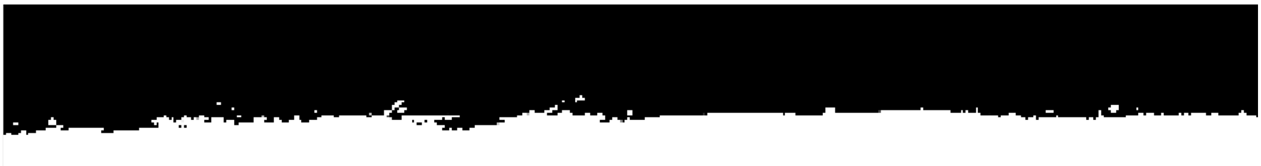

(c) Frame 20001: reconstructed with 10 mode

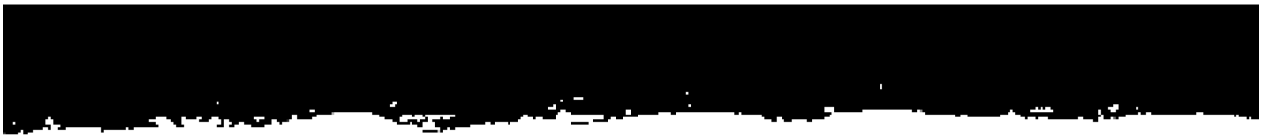

(d) Frame 20001: reconstructed with 25 mode

(e) Frame 20001: reconstructed with 50 mode

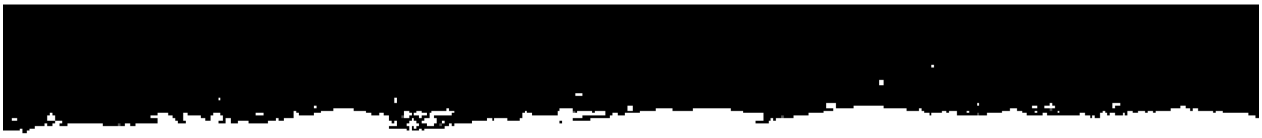

(f) Frame 20001: reconstructed with 100 mode

Figure 10: Frame 20001 of test 203, original and reconstructed

4.2 ICA Reconstruction

The ICA is a statistical technique used to reveal the independent components, hidden in the observed data. This allows the identification of the leading independent structures appearing during the burning process and representing some physical processes involved in the observed phenomenon. As said in section 2.2, before applying the ICA algorithm, the video data are first projected onto their POD modes, in order to operate on a lower-dimensional dataset that still retains the most important information and has a higher signal-to-noise ratio. According to the previous study on the energy fraction carried by each eigenvalue (see Figures 7 and 8), it is possible to state that no big differences on the main process dynamics are observed when 25, 50 or 100 modes are considered (see section 4.1). On the other hand, when the ICA is performed, important differences are found when the data are projected onto 10, 25, 50 or 100 POD modes and the same number of independent components is computed. In particular, the more the data are filtered (which means the lower the number of retained POD modes), the better the main features of the combustion process are described. This is due to the fact that samples of observations of random variables converge to a Gaussian distribution when the number of observation is sufficiently large. This means that, the larger the dataset, the more Gaussian the

DOI: 10.13009/EUCASS2019-629

variables. Since the ICA technique starts from the assumption that the analyzed variables need to be non-Gaussian, the algorithm works better when applied on a lower dimensional and less noisy dataset. In order to prove this, the video data were projected onto 10 and 100 POD modes, before computing 10 independent components. The results show that, in the first case (10 POD modes, 10 ICs), the average flame structure is recovered, while, in the second case (100 POD modes, 10 ICs) only spurious fluctuations are found, see Fig. 11. This means that either the original signal is too noisy (thus, the dataset has to be reduced to a lower dimensional system) or 10 ICs are too few to describe such a big dataset.

(a) Frame 20001: original

(b) Frame 20001: reconstructed with 10 POD modes and 10 ICs

(c) Frame 20001: reconstructed with 100 POD modes and 10 ICs

Figure 11: Frame 20001 of test 203, original and reconstructed

Of course, it is necessary to find a good balance between the right number of POD modes and ICs to compute. In fact, 10 POD modes could be enough to represent the average flame behaviour, but 10 ICs are probably too few to correctly describe the phenomenon (clearly, the number of ICs cannot be higher than the number of POD modes). Therefore, a study on the correct number of ICs was performed. When the all dataset is considered (100 POD modes) and a different number of ICs is computed, it is noticed that the results are getting closer to the original data if more ICs are considered. In this case, incoherent and filament-like structures are found when only 10 ICs are computed, while the main average flame structure is reconstructed with 100 ICs (see Fig. 12). It is also noticed that the higher the number of ICs, the flatter the flame. More fluctuations and smaller roll-waves are visible with a lower number of ICs. Unfortunately, looking at the original frame, it is possible to observe that these features are not present in the original video data. These are, most likely, spurious and noisy signals coming from the algorithm itself. This could be due to the fact that, as already underline previously, the original signal is not really non-Gaussian and the different spatial components contained in the dataset are not totally independent from each other. Moreover, as already said in section 2.2, the ICA is not able to order its components according to a defined criterion (like the POD) and it provides a solution only up to a multiplicative constant. Therefore, it is not said that the first 10 ICs are the most important sources for describing the dynamics of the process. This means that it is better to reduce the dimension of the problem at the beginning, by using the POD projection, thus being sure that only the most energetic components are retained and that the noise is filtered out, and then compute the maximum number of ICs of the system, so that all the ICs are retained (from the most to the less important). Alternatively, if no POD modes projection wants to be performed before, it is recommended to compute as many ICs as possible and to choose a posteriori which one to retain and which not.

DOI: 10.13009/EUCASS2019-629

(a) Frame 20001: original

(b) Frame 20001: reconstructed with 100 POD modes and 10 ICs

(c) Frame 20001: reconstructed with 100 POD modes and 25 ICs

(d) Frame 20001: reconstructed with 100 POD modes and 50 ICs

(e) Frame 20001: reconstructed with 100 POD modes and 100 ICs

Figure 12: Frame 20001 of test 203, original and reconstructed

5. Conclusion

In the framework of this research, the decomposition of the hybrid combustion flame into its principal and independent components was performed with POD and ICA, respectively. This allows to reduce the dimension of the problem and to find the leading structures characterizing the combustion process. In order to prove the validity of this approach, a modes reconstruction of the hybrid flame was performed in this work.

For what concerns the POD analysis, a decomposition and reconstruction of the main flame using a different number of modes was performed. In particular, it was shown that the average flame structure is already well describe by the first mode, since it retains already almost 90% of the whole energy content of the combustion process. When a higher number of modes is considered, also smaller turbulent structures and fluctuations are detected. With 50 modes, all waves and droplets are clearly recognized and the dynamics is well reproduced.

For what concerns the ICA decomposition, an analysis was done by varying the number of POD modes considered for the problem dimensionality reduction and the number of independent components. It was observed that it is better to first reduce the dimension of the problem and filter out the noise, by using the POD projection, and then compute the independent components according to what wants to be studied.

The results obtained show that the modes reconstruction provides a good representation of the original video frames and prove the validity of the decomposition methods used in the framework of this research. This means that the low-dimensional mode representation is an efficient way to correctly describe the main combustion phenomena in the combustion chamber. This analysis allow us to retain the leading structures characterizing the dynamics of the process and to filter out the noise.

DOI: 10.13009/EUCASS2019-629

Acknowledgements

This work was partially funded by the DLR project ATEK (Antriebstechnologien und Komponenten fuer Traegersysteme: Propulsion Technologies and Components for Launcher Systems). The support of the M11 team and the propellants department is greatly acknowledged.

References

[1] K. Bizon, G. Continillo, S. Lombardi, E. Mancaruso, and B.M. Vaglieco. Spatial and temporal independent component analysis of flame dynamics in diesel engine. In *XXXVI Meeting of the Italian Section of the Combustion Institute*, June 2013.

[2] K. Bizon, G. Continillo, E. Mancaruso, S.S. Merola, and B.M. Vaglieco. Pod-based analysis of combustion images in optically accessible engines. *Combustion and Flame*, 157(4):632–640, April 2010.

[3] K. Bizon, S. Lombardi, G. Continillo, E. Mancaruso, and B. M. Vaglieco. Analysis of diesel engine combustion using imaging and independent component analysis. *Proceedings of the Combustion Institute*, 34(2):2921–2931, January 2013.

[4] A. Cammilleri, F. Gueniat, J. Carlier, L. Pastur, E. Memin, F. Lusseyran, and G. Artana. POD-spectral decomposition for fluid flow analysis and model reduction. *Theoretical and Computational Fluid Dynamics*, 27(6):787–815, February 2013.

[5] Anindya Chatterjee. *An introduction to the proper orthogonal decomposition*, 2000.

[6] H. K. Ciezki, J. Sender, W. Clau-oslash, A. Feinauer, and A. Thumann. Combustion of solid-fuel slabs containing boron particles in step combustor. *Journal of Propulsion and Power*, 19(6):1180–1191, November 2003.

[7] S. Dodel, J. M. Herrmann, and T. Geisel. Comparison of temporal and spatial ica in fmri data analysis. *Proceedings of ICA 2000*, 2000.

[8] P. Hoyer and A. HyvÃ¤rinen. Independent component analysis applied to feature extraction from colour and stereo images. *Network: Computation in Neural Systems*, 11(3):191–210, January 2000.

[9] A. Hyvarinen. One-unit contrast functions for independent component analysis: a statistical analysis. *Neural Networks for Signal Processing VII. Proceedings of the 1997 IEEE Workshop*, 1997.

[10] A. Hyvarinen and E. Oja. Independent component analysis: algorithms and applications. *Neural Networks*, 13(4-5):411–430, June 2000.

[11] A. Karabeyoglu. Hybrid rocket propulsion for future space launch. In *Aero/Astro 50th Year Anniversary Stanford University*, 2008.

[12] A. Karabeyoglu, D. Altman, and B. J. Cantwell. Combustion of liquefying hybrid propellants: Part 1, general theory. *Journal of Propulsion and Power*, Vol.18(No. 3):610–620, May 2002.

[13] A. Karabeyoglu, B.J. Cantwell, and D. Altman. Development and testing of paraffin-based hybrid rocket fuels. In *37th AIAA/ASME/SAE/ASEE Joint Propulsion Conference and Exhibit*, Salt Lake City, Utah, July 2001. American Institute of Aeronautics and Astronautics.

[14] A. Karabeyoglu, Brian J. Cantwell, and Jose Stevens. Evaluation of homologous series of normal-alkanes as hybrid rocket fuels. In *41st AIAA/ASME/ASEE Joint Propulsion Conference*, July 2005.

[15] A. Karabeyoglu, J. Stevens, D. Geyzel, B. Cantwell, and D. Micheletti. High performance hybrid upper stage motor. In *47th AIAA/ASME/SAE/ASEE Joint Propulsion Conference and Exhibit*. American Institute of Aeronautics and Astronautics, July 2011.

[16] Gaetan Kerschen, Jean claude Golinval, Alexander F. Vakakis, and Lawrence A. Bergman. The method of proper orthogonal decomposition for dynamical characterization and order reduction of mechanical systems: An overview. *Nonlinear Dynamics*, 41(1-3):147–169, August 2005.

DOI: 10.13009/EUCASS2019-629

[17] M. Kobald and E. Toson. Evaluation of paraffin-based fuels for hybrid rocket engines. In *50th AIAA/ASME/SAE/ASEE Joint Propulsion Conference*. American Institute of Aeronautics and Astronautics, July 2014.

[18] M. Kobald, I. Verri, and S. Schlechtriem. Theoretical and experimental analysis of liquid layer instability in hybrid rocket engines. *CEAS Space Journal*, 7(1):11–22, January 2015.

[19] A. Petrarolo and M. Kobald. Evaluation techniques for optical analysis of hybrid rocket propulsion. *Journal of Fluid Science and Technology*, 11(4):JFST0028–JFST0028, 2016.

[20] A. Petrarolo, M. Kobald, H. K. Ciezki, and S. Schlechtriem. Principal and independent component analysis of hybrid combustion flame. *International Journal of Energetic Materials and Chemical Propulsion*, 18(1):pp. 9–29, 2019.

[21] A. Petrarolo, M. Kobald, and S. Schlechtriem. Understanding Kelvin-Helmholtz instability in paraffin-based hybrid rocket fuels. *Experiments in Fluids*, page 59:62, 2018.

[22] James V. Stone. *Independent Component Analysis. A Tutorial Introduction,*. A Brandford Book, 2004.